Journal of Operation and Automation in Power Engineering
Vol. 7, No. 1, May 2019, Pages: 129-139
http://joape.uma.ac.ir

An Isolated Off-Line High Power Factor Electrolytic Capacitor-Less LED Driver with Pulsating Output Current

A. Ghaemi, M. R. Banaei, A. Safari*

Department of Electrical Engineering, Azarbaijan Shahid Madani University, Tabriz, Iran

Abstract- *One of the most efficient lighting technologies is based on light-emitting diodes (LEDs). Common LED drivers with AC-input (50-60Hz) usually require a bulk electrolytic capacitor to decrease low-frequency ripple in the output. However, the critical element that limits the lifespan of the LED driver is the electrolytic capacitor. An isolated off-line LED driver is proposed in this paper, in which the required output capacitance is reduced so that the electrolytic capacitor can be omitted from the driver structure. The driver's configuration and controlling method provide a high input power factor. Just a single switch and therefore a single controlling IC have been used in the proposed structure. The input power factor correction is implemented utilizing a boost-based method, and a novel structure is introduced for dc/dc conversion section. Power factor correction and dc/dc conversion are performed employing a simplistic and single controlling system. The output current feeding the LEDs is a high frequency pulsating current. Calculations, simulations and experimental waveforms of a laboratory prototype are presented to confirm the validity of the proposed driver.*

Keyword: Electrolytic capacitor, LED driver, Lifespan, Power factor.

1. INTRODUCTION

A significant portion of power production at facilities is spent on lighting. Traditional light sources have some disadvantages such as low efficiency, large size, containing hazardous materials, etc [1]. Long lifetime, high efficiency, high light quality, and very low maintenance costs make LEDs a popular choice to replace the traditional lamps. LED lamps have extensive use for various applications from low brightness to high brightness illumination [2], [3]. For single-phase (50 or 60 Hz) general lighting LED drivers, it is necessary to correct the input power factor to meet the IEC 1000-3-2 Class C standards [4]. Furthermore, the U.S. energy star program mandates that the input power factor of LED drivers must be greater than 0.9 and 0.7 for commercial and residential lightings, respectively [5].

Compared with other lighting appliances, LEDs are more prone to flickering because of their low intrinsic resistance. The low-frequency ripple in the output current will cause low-frequency light flickering, which is harmful to human health [6], [7]. Two-stage LED drivers can significantly reduce the output current ripple. However, the number of elements, costs, and size of the circuit are increased and usually two separate controlling parts are required for PFC and DC/DC stages which increase the complexity of the driver. Single-stage AC input LED drivers are more efficient and can be implemented with low cost and fewer components. However, excessive low-frequency ripple in the output current makes them unsuitable to drive the LEDs. Usually, bulk electrolytic capacitors are used to decrease the output low-frequency ripple. Estimated lifetime of an electrolytic capacitor is about 5000 hours [8] and the useful lifetime of an LED is about 50000 hours [9]. The electrolytic capacitor is the most critical limiting factor for driver life [10]. Therefore, this capacitor should be removed from the structure.

Consequently, several literatures [11]-[28] have been presented to remove the electrolytic capacitor from the circuit and maximize the life time of the LED driver. A modified harmonic injection technique to decrease the output current low-frequency ripple and eliminate the electrolytic capacitor from the driver structure is presented in Ref. [11]. The driver can be implemented in a simple and cost effective manner; however, significant power factor reduction is the main drawback of this technique. Ref. [12] proposes an offline LED driver based on inverted buck converter with multiple switches

Received: 14 Oct. 2018
Revised: 09 Feb. 2019
Accepted: 09 Mar. 2019
*Corresponding author: M. R. Banaei
E-mail: m.banaei@azaruniv.ac.ir (M. R. Banaei)
Digital object identifier: 10.22098/joape.2019.5391.1404
Research Paper

connected to LED segments. It achieved a high power factor and high efficiency, however, the main impediment of this circuit is the large numbers of the employed switches that could increase the total cost and complexity. A current balancing modular driver including a master and a slave module is presented in Ref. [13]. The master and slave parts are implemented using an LLC and LC resonant converters, respectively. However, the measured power factor and the exact value of the output current ripple have not mentioned and not analyzed in this paper. A single-coupled inductor multi-output structure is proposed in Ref. [14]. There is a direct energy flow path connecting the DC-link capacitor and output capacitors to improve the efficiency of the circuit. The driver is designed with a buck-boost PFC converter cascaded with a buck converter including multiple outputs. The proposed circuit has a complex controlling process, and there is no galvanic isolation between the input and output parts. In Refs. [15-16] a semi-Flyback electrolytic capacitor-less AC/DC converter is introduced to provide small size and improved efficiency for the circuit. However, according to the presented experimental and simulated waveforms of the output current, there is a high low- frequency ripple in the output which can lead to light flickering effects. In Refs. [17-18], an active energy storage method with an additional parallel compensation stage is used to drive the LEDs; this method can achieve a high power factor and acceptable current regulation. Another unidirectional converter based on parallel current ripple cancellation approach has been presented in Ref. [19] to obtain high power factor and flicker free LED driving. However, in such structures due to the high voltage stress on the parallel or compensation stage, the implementation costs and power losses increase relatively. Some techniques based on series compensation approach is proposed in Refs. [20-22]. In Ref. [23] an electrolytic capacitor-less LED driver is presented with constant output current, including a Flyback converter for the input power factor correction part and a buck converter as an extra path for supplying the electrical power to the load.

In comparison with parallel compensation, the voltage stresses of the elements are reduced. However, the drawback of these methods is using an additional winding which is extracted from the main stage. A full bridge series ripple compensation approach employing a floating capacitor is introduced in Ref. [24]. The auxiliary winding is eliminated in this structure; however, the controlling approach is somewhat complicated.

Pulsated current driving technique has been used in some recent works. Driving LEDs with high DC current, lead to luminous saturation. For duty cycles higher than 50%, LED's output light starts to saturate [25], [26]. It should be noted that the maximum peak current of each LED must remain under the specified value regarding the LEDs datasheet [27]. In Ref. [28] a high frequency pulsating current LED driver for residential lighting is proposed. The electrolytic capacitor has been removed. However, the output current low-frequency ripple is relatively high, and also no electrical isolation is provided. In some cases, LED semiconductor terminals are accessible; thus, due to safety considerations, electrical isolation is necessary between AC input and output LEDs. This paper proposes a novel isolated LED driver configuration, with high frequency pulsating output current. Output low-frequency ripple is reduced, and no electrolytic capacitor is required. In addition to remove electrolytic capacitors from the driver's structure and creating electrical isolation as one of the crucial issues in providing users security against electric shock especially in domestic and general lighting applications, the other main advantage of the proposed structure is the reduction of the employed switches and using just a single switch, that reduces the required elements for the implementation of the control section, decreases the complexity and also the costs. The number of the employed switches for some of the mentioned modern structures are listed in table 1. As can be seen, the number of the switches in these references are higher than the proposed LED driver, which in turn could increase the complexity and cost of control implementation. The proposed structure ensures a high input power factor, which will be illustrated through the simulations and experimental results. The characteristics and operating principles of the proposed LED driver are provided and analyzed in this paper. Fig.1 shows the generic power stage diagram of the proposed circuit.

Table 1. The number the employed switches for some of the novel references

Ref.	Number of the employed switches	Ref.	Number of the employed switches
[12]	4	[18]	2
[13]	2	[19]	3
[14]	>3	[22]	6
[15]	2	[23]	2
[16]	2	[24]	6

This paper is organized as follows: The proposed topology, operating stages and related equations are discussed in section 2. Section 3 presents the design example and experimental results. Finally, the conclusion is given in section 4.

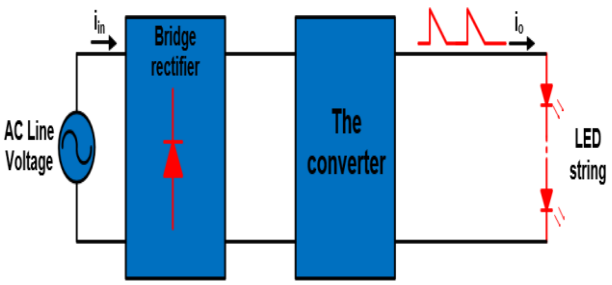

Fig. 1. Generic power stage diagram of the proposed LED driver

2. OPERATING PRINCIPLES

The proposed electrolytic capacitor-less LED driver is illustrated in Fig.2. The circuit consists of an input filter, a bridge rectifier and the converter. L_f and C_f form the input filter. L_1, D_1, D_2 and C_i provide a boosted voltage without any switch. Actually, the main switch (S), and two diodes (D_1 and D_2) turn on and off such that the voltage across C_i boosts the input voltage. The aforementioned part, corrects the input power factor in similar way to a boost converter. The transformer (T), has two major functions: first, it provides isolation between the input and output parts; and second, the magnetizing inductance of transformer in series with the switch (S), make a high frequency pulsating current at the output. The output capacitor will charge up through the diode (D_3) and the inductor (L_2). The operating stages and circuit analysis are given in the following part.

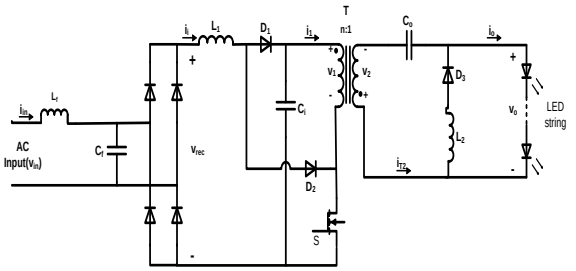

Fig. 2. The proposed LED driver

2.1 Operating stages in a switching cycle

Fig.3 illustrates the key waveforms of the proposed LED driver. The circuit operation can be analysed in three different stages as shown in Fig.4.

First stage ($t_0 < t < t_1$): The switch (S) turns on at the beginning of this stage. D_1 is off, D_2 and D_3 are conducting and LEDs are off in this stage, thus i_o=0. The input positive rectified voltage across L_1 will charge it until t_1:

$$V_{L1} = v_{rec} \tag{1}$$

The boost inductor current (L_1) can be written as:

$$i_{L1} = \frac{1}{L_1}\int_0^t v_{rec}\,dt = \frac{v_{rec}}{L_1}t \tag{2}$$

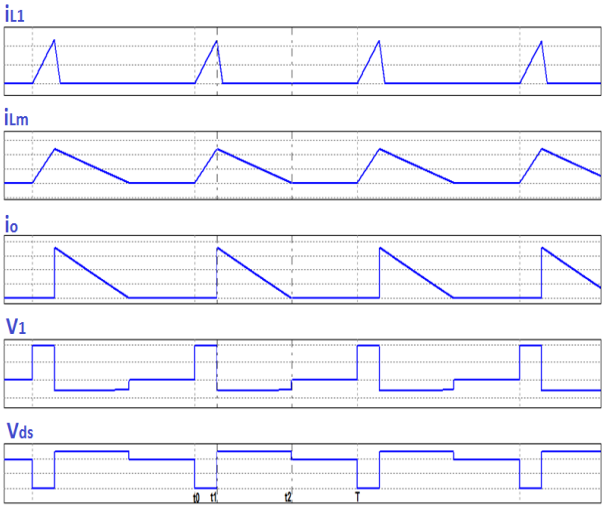

Fig. 3. Key waveforms of the proposed LED driver

The current through L_1, reaches to its peak value at the end of this stage which is equal to the peak current of D_2:

$$i_{L1,peak} = i_{D2,peak} \tag{3}$$

The time interval between 0 (t_0=0), and t_1 is equal to the ON time of the switch (DT), where D represents the duty cycle of switching. So, $i_{L1,peak}$ can be expressed as:

$$i_{L1,peak} = i_{D2,peak} = \frac{v_{rec}}{f_s L_1} D \tag{4}$$

Where f_s is the switching frequency. In Fig.4, i_{Lm} represents the current of magnetizing inductance for the transformer (T). i_1 is equal to the sum of i_{Lm} and the primary current of the transformer (i_{T1}):

$$i_1 = i_{Lm} + i_{T1} \tag{5}$$

The magnetizing inductance current can be expressed as:

$$i_{Lm} = \frac{1}{L_m}\int_0^t V_i\,dt = \frac{V_i}{L_m}t \tag{6}$$

Where V_i is the average voltage across C_i. Here V_i is a positive voltage which increases the magnetizing inductance current during this interval. Thus $i_{Lm,peak}$ will be equal to:

$$i_{Lm,peak} = \frac{V_i}{f_s L_m} D \tag{7}$$

Secondary voltage of the transformer can be written as:

$$V_2 = \frac{V_1}{n} \tag{8}$$

Where V_1=V_i and n is the turn ratio of the transformer (N_p/N_s).

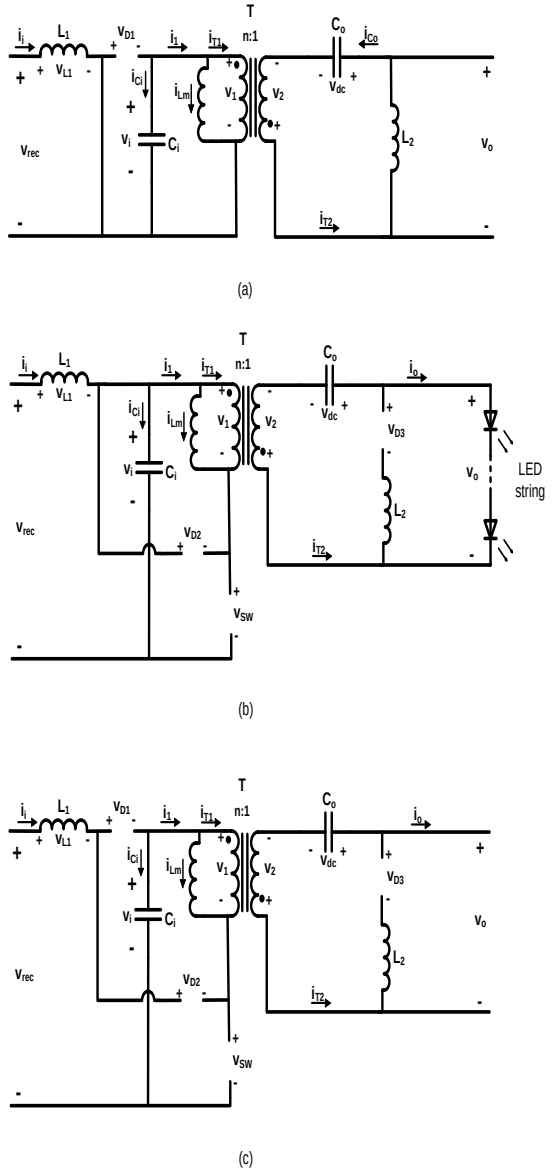

Fig. 4. Circuit operating stages: (a) $t_0 < t < t_1$, (b) $t_1 < t < t_2$, (c) $t_2 < t < T$

Applying KVL in the secondary side of transformer leads to:

$$V_{L2} = V_2 - V_{dc} = \frac{V_i}{n} - V_{dc} \tag{9}$$

V_{dc} is the average voltage across C_o. Thus, the current through L_2 can be written as:

$$i_{L2} = \frac{1}{L_2}\int_0^t (\frac{V_i}{n} - V_{dc})\,dt = \frac{1}{L_2}(\frac{V_i}{n} - V_{dc})t \tag{10}$$

This expression is equal to the charging current of C_o. The peak value of i_{L2}, as well as, i_{Co} for this stage can be obtained as:

$$i_{L2,peak} = i_{Co,peak} = \frac{1}{L_2 f_s}(\frac{V_i}{n} - V_{dc})D \tag{11}$$

Second stage ($t_1 < t < t_2$): As this stage starts, the switch turns off and i_1 drops to zero. Also, the diode D_1 turns on, and LEDs start conducting. D_2 and D_3 are off in this time interval. The peak value of the output current is an important quantity in high frequency pulsating current LED drivers. According to Fig.4(b), the output peak current can be expressed as:

$$i_{o,peak} = n i_{Lm,peak} \tag{12}$$

The peak value of the magnetizing inductance current can be obtained from Eq. (7). Thus:

$$i_{o,peak} = \frac{V_i}{f_s L_m} nD \tag{13}$$

The voltage across L_m can be found using Eq. (14) and then $i_{Lm}(t)$ can be expressed as Eq. (15).

$$V_{Lm} = nV_2 = n(V_{dc} - V_o) \tag{14}$$

$$i_{Lm} = \frac{1}{L_m}\int_{DT}^{t} n(V_{dc} - V_o)\,dt + \frac{V_i}{L_m}DT \tag{15}$$

The time interval between t_1 and t_2 is represented by $D'T$, which shows the discharge time of i_{Lm}. As time passes in this stage, the magnetizing inductance current decreases and eventually reaches to zero at t_2. Evaluating Eq. (15) at $t=t_2$ and noting that $t_2=(D+D')T$, D' can be found as:

$$D' = \frac{V_i D}{n(V_o - V_{dc})} \tag{16}$$

In this stage, V_{L1} is given by the difference between v_{rec} and V_i. V_i is greater than the rectified voltage. Therefore, the voltage across L_1 will be negative in this stage. This voltage discharges L_1 until t_2. The relation between v_{rec} and V_i can be obtained using the volt-second balance principle for L_1 as Eq. (17). Fig.5 illustrates the voltage across L_1 in a switching cycle.

$$v_{rec}(DT) + (v_{rec} - V_i)(D''T) = 0 \tag{17}$$

The second operating stage can be divided into two sub-stages: 1. When i_{L1} is decreasing and 2. After i_{L1} reaches to zero. $D''T$, shows the time required for discharging L_1 from its peak value to zero. In this time interval, i_{L1} can be found as:

$$i_{L1} = \frac{1}{L_1}\int_{DT}^{t}(v_{rec} - V_i)\,dt + i_{L1}(DT) \tag{18}$$

$$i_{L1} = \frac{v_{rec} - V_i}{L_1}(t - DT) + \frac{v_{rec}D}{f_s L_1} \tag{19}$$

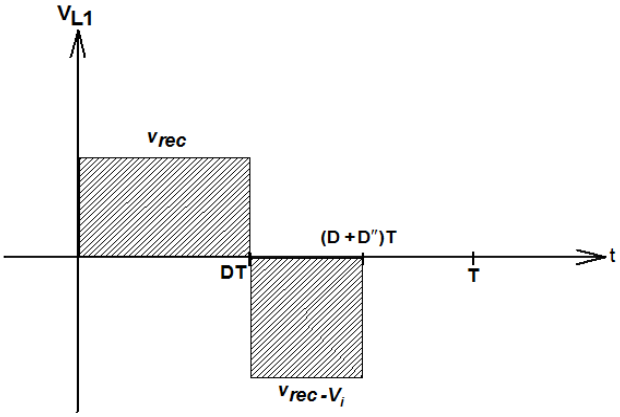

Fig. 5. The voltage across L_1 in a switching period

Because of DCM operation of L_1, i_{L1} reaches to zero at t=(D+D″)T. By evaluating Eq. (19) at t=(D+D″)T, D″ can be obtained as:

$$D'' = (\frac{v_{rec}}{V_i - v_{rec}})D \tag{20}$$

Using (4), the above relation can be rewritten as Eq. (21). Assuming that $i_{D2,avg}=D(i_{L1,peak}/2)$, D″ can be expressed as (22).

$$D'' = \frac{f_s L_1 i_{L1,peak}}{V_i - v_{rec}} \tag{21}$$

$$D'' = \frac{2 f_s L_1 i_{D2,avg}}{D(V_i - v_{rec})} \tag{22}$$

Third stage (t_2 < t < T): As shown in Fig. 4(c), the switch, all of the diodes and LEDs are off in this stage; thus i_i=0, i_1=0, and i_o=0. This period ends at t=T.

2.2. Calculating the voltage across C_o(V_{dc})

First of all, the relation between V_i and V_{dc} should be calculated. Input capacitor (C_i) charges up in the first operating stage and discharges in the next one. The current through C_i at (t_0 < t < t_1) is equal to -i_1 which can be obtained using (5), (6) and (10). The relation in (23) expresses the result for i_{Ci}. On the other hand, i_{Ci} for the interval of (t_1 < t < t_2) is equal to i_{L1} which is given by (19).

$$i_{C_i} = -(\frac{V_i}{L_m} + \frac{1}{L_2 n}(\frac{V_i}{n} - V_{dc}))t \ , \ 0 < \ t \ < DT \tag{23}$$

According to Eq. (23) and Eq. (19), the absolute peak value of i_{Ci} for (t_0 < t < t_1) can be found as Eq. (24); also the peak value of i_{Ci} for (t_1 < t < t_2) is equal to $i_{L1,peak}$, which is given in Eq. (25).

$$i_{C_i,peak} = (\frac{V_i}{L_m} + \frac{1}{L_2 n}(\frac{V_i}{n} - V_{dc}))DT \ , \ 0 < \ t \ < DT \tag{24}$$

$$i_{C_i,peak} = \frac{v_{rec}D}{f_s L_1} \quad , \quad DT < \ t \ < (D + D')T \tag{25}$$

Fig.6(a) shows i_{Ci} in a switching cycle; according to the charge balance principle of the capacitor, two illustrated areas must be equal. Thus, the relationship between V_{dc} and V_i can be obtained from Eq. (26).

$$V_{dc} = -\frac{{v_{rec}}^2}{V_i - v_{rec}} \times \frac{L_2 n}{L_1} + V_i(\frac{L_2 n}{L_m} + \frac{1}{n}) \tag{26}$$

Fig.6(b) shows the current waveform of C_o in a switching cycle. The current passing through C_o for the time intervals of (t_0 < t < t_1), and (t_1 < t < t_2) is equal to i_{L2} and i_o, respectively, which i_o=ni_{Lm}. Then the peak values of i_{L2} and i_o for the specified intervals could be found using Eq. (11) and Eq. (13), respectively. According to Fig.6(b), and the charge balance principle for C_o, another relation between V_{dc} and V_i can be obtained as Eq. (27).

$$V_{dc} = \frac{V_i L_m + nL_m V_o - \sqrt{(V_i L_m + nL_m V_o)^2 - 4(nL_m)(V_i L_m Vo - nL_2 {V_i}^2)}}{2nL_m}$$

(1)

V_o is equal to the sum of LEDs forward voltages. To obtain the value of V_{dc}, the value of V_i should be found at first. Substituting Eq. (27) in Eq. (26) provide a new relation in term of V_i as:

$$\frac{V_i L_m + nL_m V_o - \sqrt{(V_i L_m + nL_m V_o)^2 - 4(nL_m)(V_i L_m Vo - nL_2 V_i^2)}}{2nL_m}$$
$$+ \frac{{v_{rec}}^2}{V_i - V_{rec}} \times \frac{L_2 n}{L_1} - V_i(\frac{L_2 n}{L_m} + \frac{1}{n}) = 0$$

(2)

As expressed in Eq. (29) a fourth-degree equation will be obtained for V_i. Solving this equation and substituting its solution in Eq. (26), returns the value of V_{dc}.

$$a_4 V_i^4 + a_3 V_i^3 + a_2 V_i^2 + a_1 V_i^1 + a_0 = 0 \tag{29}$$

Where:

$$a_4 = a^2 - c$$
$$a_3 = -2a^2 vrec + 2anL_m V_o - d$$
$$a_2 = a^2 v_{rec}{}^2 + (nL_m V_o)^2 + 2ab - 4anL_m V_o v_{rec} - e$$
$$a_1 = -2v_{rec}((nL_m V_o)^2 + ab) + 2nV_o L_m (av_{rec}{}^2 + b) - f$$
$$a_0 = b^2 - 2bnL_m V_o v_{rec}$$

And:

$$a = L_m(1 - 2n(\frac{L_2 n}{L_m} + \frac{1}{n})),\quad b = 2nL_m v_{rec}{}^2 \frac{L_2 n}{L_1}$$
$$c = L_m{}^2 + 4n^2 L_m L_2,\ d = -2L_m{}^2(v_{rec} + nV_o) - 8n^2 L_m L_2 v_{rec}$$
$$e = L_m{}^2((V_o + v_{rec})^2 + 2nV_o v_{rec}) + 4n^2 L_m L_2 v_{rec}{}^2$$
$$f = -2nL_m{}^2 V_o v_{rec}(v_{rec} + nV_o)$$

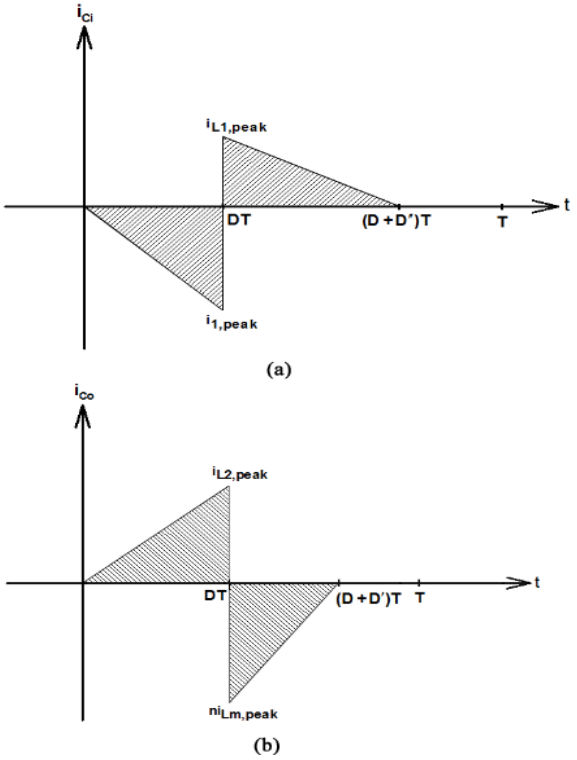

Fig. 6. Waveform of the currents passing through: (a) the C_i (b) the C_o

2.3. Average value of i_{L1} in a switching cycle

The input current value ($i_{in}(\theta)$) is the same with the average value of i_{L1} in a switching cycle ($i_{L1,avg}$). Since $f_s >> f_L$, the line current can assume to be constant in a switching cycle (f_L is the line frequency). To find the average value of i_{L1}, it should be noted that $i_{L1,avg}$ has two different parts:

$$i_{L1,avg} = i_{D1,avg} + i_{D2,avg} \tag{30}$$

$i_{L1}(t)$ for ($0 < t < DT$) and ($DT < t < (D + D'')T$) can be obtained using Eq. (2) and Eq. (19), respectively. $i_{D2,avg}$ can easily be found as:

$$i_{D2,avg} = \frac{v_{rec} D^2}{2 f_s L_1} \tag{31}$$

The average current flowing D_1 can be defined by Eq. (32). Substituting Eq. (20) into Eq. (32), will result in Eq. (33), and according to (30) the final value of $i_{L1,avg}$ can be obtained as Eq. (34).

$$i_{D1,avg} = \frac{1}{T}\int_{DT}^{(D+D'')T} (\frac{v_{rec} - V_i}{L_1}(t - DT) + \frac{v_{rec} D}{f_s L_1})dt \tag{32}$$

$$i_{D1,avg} = \frac{v_{rec}{}^2 D^2}{2 f_s L_1 (V_i - v_{rec})} \tag{33}$$

$$i_{L1,avg} = \frac{D^2}{2 f_s L_1}(\frac{v_{rec} V_i}{V_i - v_{rec}}) \tag{34}$$

Now the rms value of the input current can be defined as Eq. (35). Substituting Eq. (34) into Eq. (35), will result in (36).

$$i_{in,rms} = \sqrt{\frac{1}{\pi}\int_0^{\pi} i_{in}{}^2(\theta) d\theta} \tag{35}$$

$$i_{in,rms} = \frac{D^2}{2 f_s L_1}\sqrt{\frac{1}{\pi}\int_0^{\pi}(v_{rec}(\frac{V_i}{V_i - v_{rec}}))^2 d\theta} \tag{36}$$

Where for a half line cycle, v_{rec} can be assumed as:

$$v_{rec} = v_m \sin\theta \tag{37}$$

2.4. Output capacitance (C_o) calculation

To further decrease the output low-frequency ripple, the output capacitance should be increased; however, to remove the electrolytic capacitor form driver's structure, the capacitance must be reduced. Peak to peak voltage ripple across the output capacitor is given by:

$$V_{dc-r} = \frac{P_{in,avg}}{C_o V_{dc}\omega} = \frac{P_{in,avg}}{C_o \times V_{dc} \times 2\pi \times (2 f_L)} \tag{38}$$

Where $P_{in,avg}$ is the average value of the input power. Thus, the required output capacitance can be expressed as:

$$C_o = \frac{P_{in,avg}}{V_{dc-r} \times V_{dc} \times (4\pi f_L)} \tag{39}$$

2.5. Input power factor

A high input power factor can be achieved in the proposed LED driver. Power factor correction (PFC) in this circuit is similar to the boost PFC converter operation in discontinuous conduction mode; however, it should be noted that the PFC and the output current regulation are

done just by a single switch. Input power factor relation can be expressed as Eq. (40).

$$PF = \frac{P_{in,avg}}{v_{in,rms} \times i_{in,rms}} \tag{40}$$

Where $v_{in,rms}$ is the effective value of the input line voltage which easily can be found as $v_m/\sqrt{2}$. v_m is the peak value of the input voltage. Average input power can be expressed as Eq. (41). Assuming $v_{in} = v_m \sin\theta$ and substituting Eq. (35) into Eq. (41), $P_{in,avg}$ can be obtained as Eq. (42).

$$P_{in,avg} = \frac{1}{\pi}\int_0^{\pi} v_{in}(\theta) i_{in}(\theta)\, d\theta \tag{41}$$

$$P_{in,avg} = \frac{D^2 v_m{}^2 V_i}{2 f_s L_1 \pi}\int_0^{\pi} \left(\frac{\sin^2(\theta)}{V_i - v_{rec}}\right) d\theta \tag{42}$$

Substituting Eq. (36) and Eq. (42) into Eq. (40), and simplifying it; the final relation for the input power factor can be obtained as:

$$PF = \frac{\frac{\sqrt{2}}{\pi}\int_0^{\pi} \left(\frac{\sin^2(\theta)}{V_i - v_{rec}}\right) d\theta}{\sqrt{\frac{1}{\pi}\int_0^{\pi} \left(\frac{\sin(\theta)}{V_i - v_{rec}}\right)^2 d\theta}} \tag{43}$$

According to Eq. (43), changing the value of V_i will alter the power factor of the circuit, so V_i must be selected such that a high power factor could be achieved.

2.6. Voltage stress across the switch

The maximum voltage stress on the switch (S) will occur when the diode D_1 and LEDs are conducting, and D_2, D_3, and the switch are off (i.e., the second operation stage).

According to Fig .4(b), V_{sw} can be obtained as:

$$V_{sw} = V_i - V_1 \tag{44}$$

Assuming $V_1 = nV_2$ and substituting Eq. (14) into Eq. (44), maximum voltage stress across the switch can be described as follows:

$$V_{sw} = V_{i,\max} + n(V_o - V_{Co}) \tag{45}$$

2.7. Controlling the output current

A simple controlling approach is utilized in this paper to control and limit the peak value of the output current. The output peak current should be kept under the mentioned specified value in LEDs datasheet. To regulate the output current, the voltage across the input capacitor (V_{Ci}) is measured at first, and then the duty cycle of switching is calculated according to (13). To further simplify the relation, Eq. (13) can be written as:

$$D = \frac{i_{o,peak} f_s L_m}{n V_i} \tag{46}$$

The resulted duty cycle prevents overdriving of LEDs by limiting $i_{o,peak}$ in a switching period. No feedback signal is used from the secondary part to control the current, that enables a simple implementation for the control section. As shown in Figure 7, a microcontroller (LPC1768) has been used to implement the control section of the circuit. The measured voltage by the sensor is given as a physical input to the microcontroller. Also, the maximum allowed duty cycle to prevent an increase in the output current from the permissible limit is given to the microcontroller through the software codes. This value will be obtained according to the following discussions and specifications of the selected LED. The microcontroller has been programmed to receive the value of V_i, and then calculate the value of duty cycle employing the relation (46). If the calculated value for D is inside the allowable range (i.e., less than D_{max}), the microcontroller will apply the switching pulses to the circuit with a predefined frequency. If for a moment the calculated D exceeds D_{max}, the duty cycle will be set to D_{max}. Also, it should be noted that a resistive voltage divider and analog to digital part of the microcontroller could be used instead of the voltage sensor. This method increases the complexity of programming and decreases the relative accuracy, however, on the other hand, it reduces the implementation cost of the control circuit.

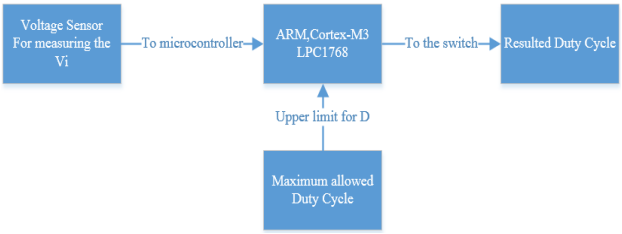

Fig. 7. The general block diagram of the control system

3. DESIGN EXAMPLE AND EXPERIMENTAL RESULTS

A 24.2W prototype is simulated and constructed to verify the validity of the proposed LED driver. The circuit is simulated in PSIM. The driver uses the line voltage (220Vrms) as input. The switching frequency is 100kHz. The ON time portion for LEDs (D′) is lower than 50%, thus according to [27], $i_{o,peak}$ can be increased up to 200% of the maximum DC rated current of LEDs. The parameters and component values of the proposed driver are given in Table 2.

The voltage drop of the selected LEDs is 36V for each one, and 8 LEDs are connected in series. Therefore, the

total forward voltage of the LED string will be equal to 288V(DC). Maximum rated DC current of the LEDs is 175mA [29], thus with D' under 50%, the peak value of the output pulsating current can be 350mA. If it is assumed that the value of $i_{o,avg}$ is approximately equal to $D'(i_{o,peak}/2)$, with a maximum value of 48% for D', $i_{o,avg}$ will be about 84mA. The proceeding information will result in the output power of 24.2w.

Table 2. Prototype specifications

Transformer turn ratio (N_p:N_s)	3:2
Magnetizing inductance (L_m)	2.2mH
Input inductor(L_1)	0.7mH
Output inductor(L_2)	7uH
Capacitor (C_i)	5uf
Line frequency (f_L)	50Hz
Driver output voltage (V_o)	288V
LED load	MHBAWT-000N0HC227G
MOSFET (S)	IPP80R450P7XKSA1, 800V
Diodes (D_1, D_2, D_3)	1N4937RLG, Fast Recovery
Filter capacitor (C_f)	50nf
Filter inductor (L_f)	2.2mH
Output capacitor (C_o)	6.8uf

Assuming a minimum efficiency of 85% for the proposed circuit, the average input power can be found to be 28.46w. According to Eq. (43) the power factor is affected by V_i. V_i is selected to be 375V in this circuit; from Eq. (43) the theoretical power factor for this voltage will be equal to 0.945. From Eq. (12), the peak value of the magnetizing inductance current is obtained to be 233mA. With a maximum value of 20% for duty cycle and using Eq. (7), the value of magnetizing inductance will be around 2.2mH. The peak value of i_{L2} is equal to the peak value of i_{Co} (at $(t_0 < t < t_1)$); actually, L_2 is used to limit the peak value of i_{Co} (while C_o is charging). On the other hand, the value of L_2 should be small enough, so that i_{L2} immediately drops to zero and D_3 could turn off after the switch. L_2 is selected to be 7uH. Now, according to Eq. (27), V_{dc} is calculated to be 240V.

According to Eq. (36), the rms value of the input current, ($i_{in,rms}$) can be found to be 0.135A; then using Eq. (40), the average input power is calculated to be 28.1W, which result in an efficiency of 86.1%. Eq. (39) is used to find the minimum required capacitance of C_o. By allowing a 30V peak to peak ripple in V_{dc}, the minimum value of C_{dc} can obtain to be 6.2uf. The final value of C_{dc} is selected to be 6.8uf. According to Eq. (45), the voltage stress on the switch will be around 465V.

Fig. 8(a) illustrates the simulated output current and the high frequency pulsating waveform of i_o is shown in Fig. 8(b). It can be seen that the peak value of output current is limited to 350mA. Also there is a little low-frequency ripple on i_o, (less than 10%). The output voltage is shown in Fig. 8(c) and a detailed view of V_o is indicated in Fig. 8(d). As can be seen from the last figure, the voltage across the LEDs is around 288V while they are conducting (second operating stage), after that (third operating stage) i_o=0 (and i_{T2}=0) and V_o is equal to V_{Co}. The voltage across LEDs is zero in the first operating stage.

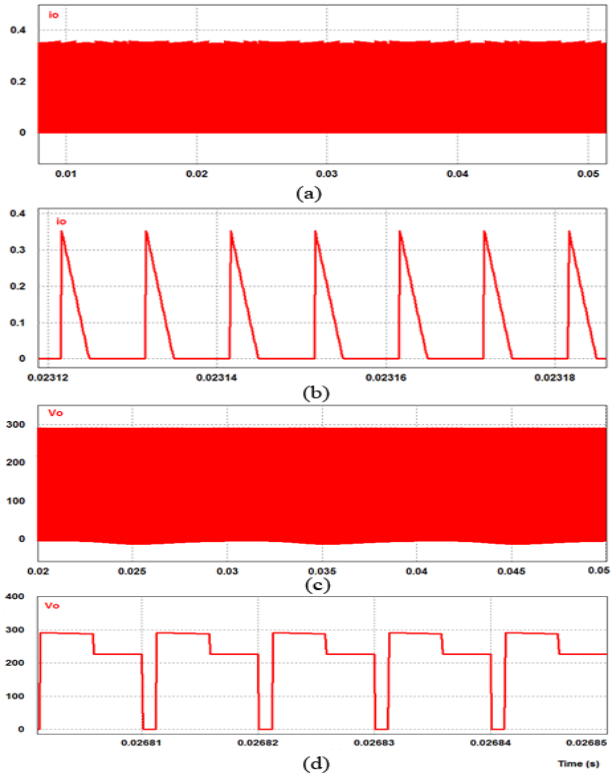

Fig. 8. (a) Output current (b) High frequency pulsating waveform of i_o (c) Output voltage (d) Detailed view of V_o

Fig. 9(a) shows the waveform of the input current, the obtained rms value of i_{in} is 0.13A. According to Fig. 9(a) the input power factor of the circuit is 0.95. The current passing through L_1 is shown in Fig. 9(b) and (c). The peak value of i_{L1} in each switching cycle varies with the amplitude of the input voltage, which results in a high input power factor. It should be noted that the rising part of i_{L1} is equal to i_{D2} and the descending part is the same with i_{D1}. Fig. 9(d) and (e) show the current of magnetizing inductance. The peak value of i_{Lm} is equal to $i_{o,peak}$ divided by transformer turn ratio (n), thus as can be seen in Fig. 9(e), $i_{Lm,peak}$ is about 233mA.

Fig. 10(a) shows the voltage across C_o. Peak to peak voltage ripple of C_o is 24V, and the average value of V_{Co} is 241V. Note that, V_{Co} does not directly apply to the LED load. The voltage across C_i is shown in Fig. 10(b); peak to peak voltage ripple of C_i is 35V, and the average value of V_{Ci} is about 375V. Fig. 10(c) and (d) show the voltage stress across the switch. As can be seen from Fig. 10(d), the voltage across the switch will be near zero while the

switch is in ON state (first operating stage). V_{sw} for the OFF state of the switch can be found using Eq. (45); which is the maximum voltage stress across the switch (second operating stage). At last (in the third operating stage), V_{sw} will be equal to V_{Ci}.

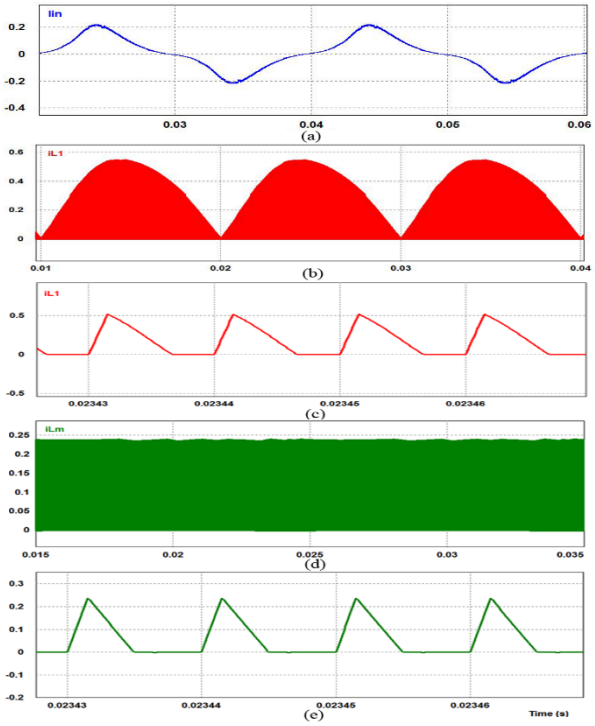

Fig. 9. (a) Input current (b) Current waveform of L1 (c) Detailed view of i_{L1} (d) Current waveform of L_m (e) Detailed view of i_{Lm}

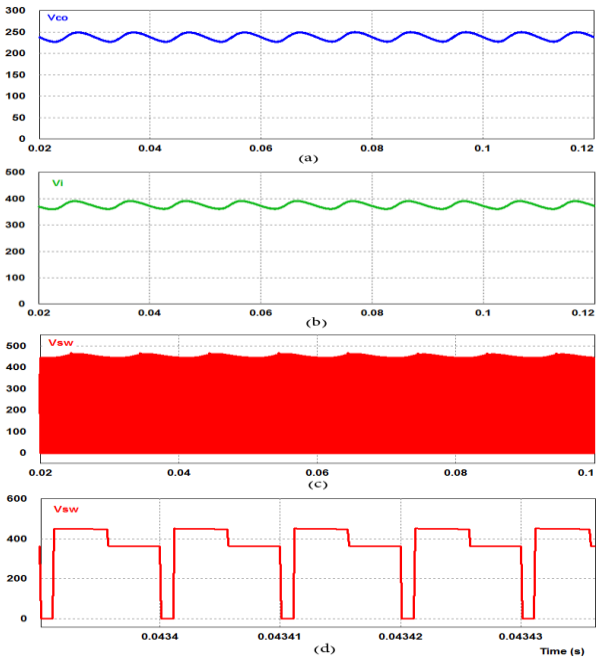

Fig. 10. (a) Voltage across the output capacitor (b) Voltage across C_i (c) Voltage stress across the switch (d) Detailed view of V_{sw}

According to the designed LED driver, a prototype has been built and tested successfully. Fig. 11 shows the measured experimental waveforms of the proposed driver. The output current and voltage, the current passing L_1, the voltage across C_i and C_o, the voltage stress across the switch and the input voltage and current are presented in Fig. 11.

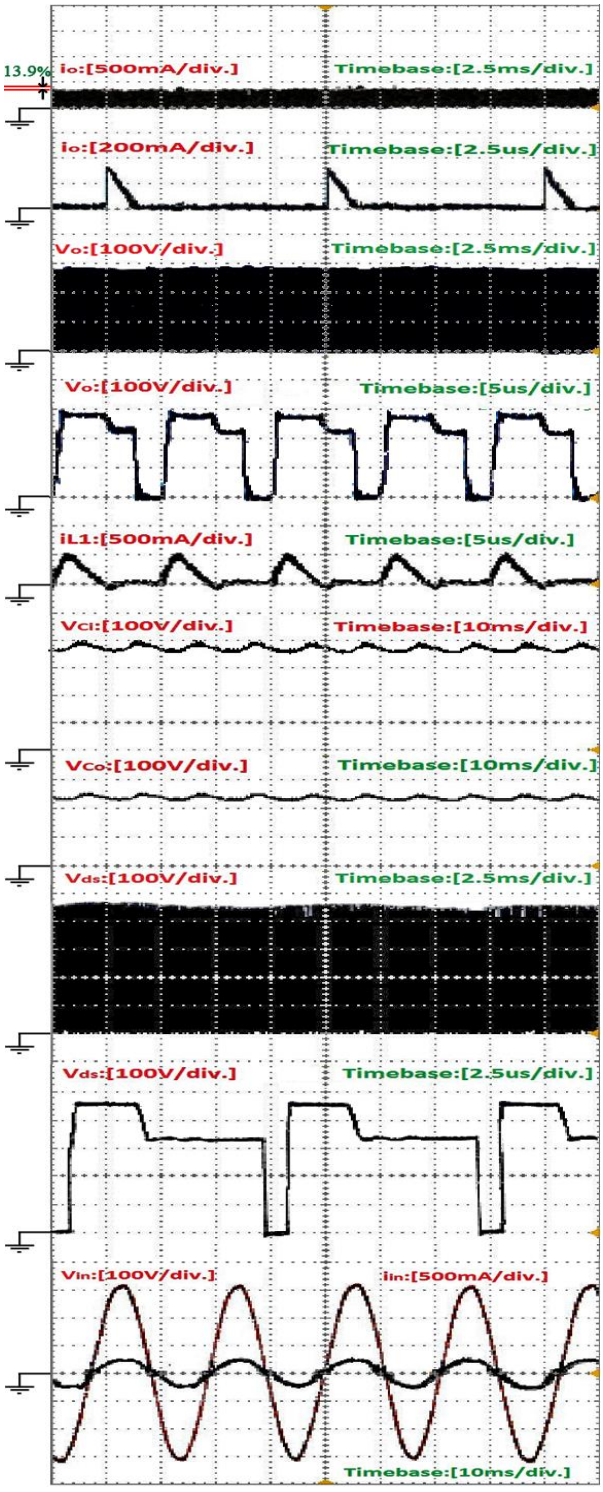

Fig. 11. Experimental waveforms of the prototype

The total time interval for the illustrated waveform of the output current is equal to a few line cycles. The low-frequency ripple of the current through the LEDs is measured to be 13.9%. The peak to peak voltage ripple

value is around 35V for V_{Ci} and 25V for V_{Co}. The maximum voltage stress across the switch is measured to be around 470V.

The measured power factor of the constructed circuit is 0.948 which is in good agreement with the proceeding analysis and simulation results. The maximum voltage stress across the switch (or switches) for the proposed circuit and some recent structures are shown in Fig.12. These values show the voltage stress across the switches in the same conditions (regarding the input voltage and the voltage of the DC link). As can be seen, the proposed circuit has a better position in this comparison. With the measured input power of 28.1w and output power of 24.2w, the efficiency of the driver will be equal to 86.1%. Fig.13 shows the photograph of the prototype.

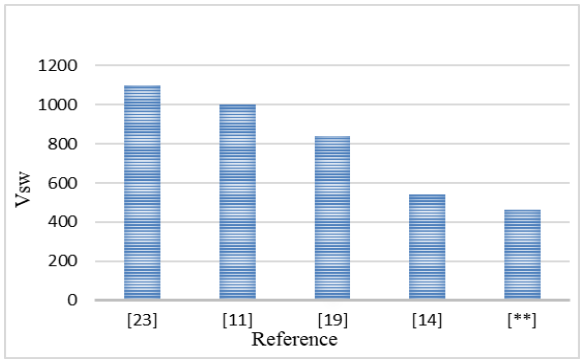

Fig. 12. Voltage stress comparison (the ** sign shows the voltage stress for the proposed circuit)

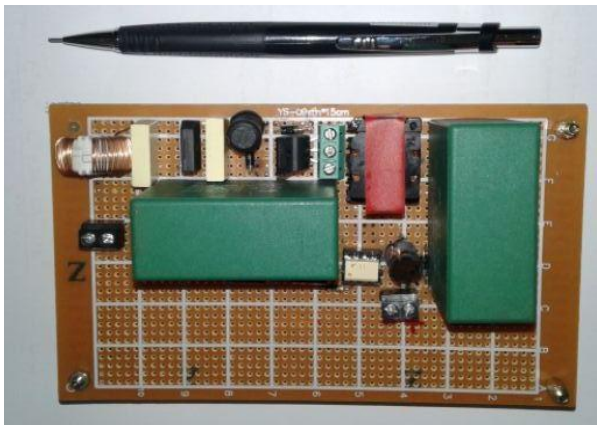

Fig. 13. Photograph of the prototype

4. CONCLUSIONS

This paper has proposed an innovative isolated LED driver with high frequency pulsating driving current. The driver ensures a high input power factor and low, output low-frequency ripple which is illustrated over the simulations and experimental results of the paper. Reduction of the output low-frequency ripple, make it possible to remove the electrolytic capacitor from the driver structure; by eliminating the electrolytic capacitor the lifetime of the proposed LED driver better matches the lifetime of LED semiconductors. The PFC action and output current regulation have done just by using a single switch and a simple controlling approach. The operating stages, calculations and detailed analysis of the proposed LED driver have been discussed in this paper.

Design example has been provided, and an experimental prototype has been built to verify the validity of the proposed LED driver. The implemented circuit is a 24.2w, 288V(DC output) driver with 220V, 50Hz AC input.

REFERENCES

[1] D. A. Steigerwald *et al.*, "Illumination with solid state lighting technology," *IEEE J. Sel. Top. Quantum Electron.*, vol. 8, no. 2, pp. 310–320, 2002.

[2] Haijin Liao, Yonghai Yu, and Xiaojian Liu, "The research of humanized design of the LED landscape lighting lamp," *2009 IEEE 10th Int. Conf. Comput-Aided. Ind. Design Conceptual Des.*, 2009, pp. 499–502.

[3] D.-H. Yoo and G.-Y. Jeong, "LCD panel sector-dimming controlled high efficiency LED backlight drive system," *2009 Int. Conf. Electr. Mach. Syst.*, 2009, pp. 1–6.

[4] "International standard IEC 1000-3-2 Class C. LED," Mar-1995.

[5] E. Energy Star, "ENERGY STAR ® Program Requirements for Solid State Lighting Luminaires."

[6] B. Lehman, A. Wilkins, S. Berman, M. Poplawski, and N. Johnson Miller, "Proposing measures of flicker in the low frequencies for lighting applications," *2011 IEEE Energy Convers. Congress Exposition*, 2011, pp. 2865–2872.

[7] A. Wilkins, J. Veitch, and B. Lehman, "LED lighting flicker and potential health concerns: IEEE standard PAR1789 update," *2010 IEEE Energy Convers. Congress Exposition*, 2010, pp. 171–178.

[8] Evox Rifa electrolytic capacitors, "Electrolytic Capacitors Application Guide," Espoo, Finland, 2001.

[9] "Lifetime of White LEDs, Energy Efficiency and Renewable Energy," *U.S.Dept. Energy*, Washington DC, 2009.

[10] L. Han and N. Narendran, "An Accelerated Test Method for Predicting the Useful Life of an LED Driver," *IEEE Trans. Power Electron.*, vol. 26, no. 8, pp. 2249–2257, Aug. 2011.

[11] M. Nassary, M. Orabi, E. M. Ahmed, E. S. Hasaneen, and M. Gaafar, "Modified harmonic injection technique for electrolytic capacitor-less LED driver," *2017 19th Int. Middle-East Power Syst. Conf. MEPCON 2017 - Proc.*, vol. 2018–Febru, no. December, pp. 1459–1464, 2018.

[12] J. Baek and S. Chae, "Off-line buck LED driver for series connected LED segments," *Conf. Proc. - IEEE Appl. Power Electron. Conf. Expo. - APEC*, pp. 1506–1510, 2017.

[13] Hyun-Su Gu and Sang-Kyoo Han, "A current-balancing modular driver for multi-channel LEDs," *8th IET Int. Conf. Power Electron. Mach. and Drives (PEMD 2016)*, Glasgow, 2016, pp. 1-6.

[14] H. Wu, S. C. Wong, and C. K. Tse, "A More Efficient PFC Single-Coupled-Inductor Multiple-Output Electrolytic Capacitor-less LED Driver With Energy-Flow-Path Optimization," *IEEE Trans. Power Electron.*, vol. PP, no. c, pp. 1–1, 2018.

[15] H.-Y. Park, B.-J. Seo, K.-S. Park, K.-S. Kang, and E.-C. Nho, "Electrolytic capacitor-less high-brightness LED

driving AC/DC converter for LED performance degradation reduction," *Electron. Lett.*, vol. 54, no. 10, pp. 648–649, 2018.

[16] K. Park, B. Seo, K. Kang, and E. Nho, "An AC-DC Power Converter for Electrolytic Capacitor-less LED Driver with High Luminous Efficacy," *2018 Int. Power Electron. Conf. (IPEC-Niigata 2018 -ECCE Asia)*, pp. 922–926, 2018.

[17] B. White, Y. F. Liu, and X. Liu, "A control technology to achieve a low cost flicker-free single stage LED driver with power factor correction," *2015 IEEE 16th Work. Control Model. Power Electron. COMPEL 2015*, 2015.

[18] Q. Hu and R. Zane, "Minimizing Required Energy Storage in Off-Line LED Drivers Based on Series-Input Converter Modules," *IEEE Trans. Power Electron.*, vol. 26, no. 10, pp. 2887–2895, Oct. 2011.

[19] P. Fang, W. Sam, Y. F. Liu, and P. C. Sen, "Single-stage LED Driver Achieves Electrolytic Capacitor-less and Flicker-free Operation with Unidirectional Current Compensator," *IEEE Trans. Power Electron.*, vol. 8993, no. c, 2018.

[20] P. Fang and Y. F. Liu, "Single stage primary side controlled offline flyback LED driver with ripple cancellation," in *2014 IEEE Appl. Power Electron. Conference and Exposition - APEC 2014*, 2014, pp. 3323–3328.

[21] P. Fang, B. White, C. Fiorentino, and Y.-F. Liu, "Zero ripple single stage AC-DC LED driver with unity power factor," in *2013 IEEE Energy Convers. Congress Exposition.*, 2013, pp. 3452–3458.

[22] Y. Qiu, H. Wang, Z. Hu, L. Wang, Y.-F. Liu, and P. C. Sen, "Electrolytic-capacitor-less high-power LED driver," in *2014 IEEE Energy Convers. Congress Exposition (ECCE)*, 2014, pp. 3612–3619.

[23] H. Valipour, G. Rezazadeh, and M. R. Zolghadri, "Flicker-free electrolytic capacitor-less universal input offline LED driver with PFC," *IEEE Trans. Power Electron.*, vol. 31, no. 9, pp. 6553–6561, 2016.

[24] Y. Qiu, L. Wang, Y.-F. Liu, and P. C. Sen, "A novel bipolar series Ripple compensation method for single-stage high-power LED driver," in *2015 IEEE Appl. Power Electron.Conf. Exposition (APEC)*, 2015, pp. 861–868.

[25] S. Buso, G. Spiazzi, M. Meneghini, and G. Meneghesso, "Performance Degradation of High-Brightness Light Emitting Diodes Under DC and Pulsed Bias," *IEEE Trans. Device Mater. Reliab.*, vol. 8, no. 2, pp. 312–322, Jun. 2008.

[26] M.-S. Lin and C.-L. Chen, "An LED Driver With Pulse Current Driving Technique," *IEEE Trans. Power Electron.*, vol. 27, no. 11, pp. 4594–4601, Nov. 2012.

[27] A. Note, "Application note: Pulsed Over-Current Driving of Cree ® XLamp ® LEDs: Information and Cautions Introduction," pp. 1–11, 2016.

[28] J. C. W. Lam and P. K. Jain, "A high power factor, electrolytic capacitor-less AC-input LED driver topology with high frequency pulsating output current," *IEEE Trans. Power Electron.*, vol. 30, no. 2, pp. 943–955, 2015.

[29] "Cree ® XLamp ® MHB-A LEDs," *Prod. Fam. data sheet*, 2017.